Research article

# Unveiling antioxidant capacity of standardized chitosan-tripolyphosphate microcapsules containing polyphenol-rich extract of *Portulaca oleraceae*

Lokot Donna Lubis [a],[*], Arya Tjipta Prananda [b], Nur Aira Juwita [c], Muhammad Amin Nasution [d], Rony Abdi Syahputra [e], Sumaiyah Sumaiyah [f],[g], Rodiah Rahmawaty Lubis [h], Muhammad Fauzan Lubis [c], Ririn Astyka [c], Jihan Firyal Atiqah [i]

[a] *Department of Histology, Faculty of Medicine, Universitas Sumatera Utara, Medan, 20155, Indonesia*
[b] *Department of Surgery, Faculty of Medicine, Universitas Sumatera Utara, Medan, 20155, Indonesia*
[c] *Department of Pharmaceutical Biology, Faculty of Pharmacy, Universitas Sumatera Utara, Medan, 20155, Indonesia*
[d] *Department of Pharmaceutical Chemistry, Faculty of Pharmacy, Universitas Muslim Nusantara Al Washliyah, Medan, Indonesia*
[e] *Department of Pharmacology, Faculty of Pharmacy, Universitas Sumatera Utara, Medan, 20155, Indonesia*
[f] *Department of Pharmaceutical Technology, Faculty of Pharmacy, Universitas Sumatera Utara, Medan, 20155, Indonesia*
[g] *Nanomedicine Center of Innovation, Universitas Sumatera Utara, Medan, 20155, Indonesia*
[h] *Department of Opthalmology, Faculty of Medicine, Universitas Sumatera Utara, Medan, 20155, Indonesia*
[i] *Bachelor Program, Faculty of Pharmacy, Universitas Sumatera Utara, Medan, 20155, Indonesia*

## ARTICLE INFO

## ABSTRACT

The medicinal plant *Portulaca oleraceae* has a long history of usage in traditional medicine. Plant extracts have several interesting pharmacological effects but have some drawbacks that can be addressed via capsulation with chitosan. This work set out to do just that tally up the antioxidant effects of a polyphenol-rich *P. olerace* extract and see how capsulation affected them. The reflux extraction and response surface methodology (RSM) were carried out to optimize the phenolic and flavonoid content of *P. oleraceae* extract. Additionally, high-resolution mass spectrometry was employed to determine the secondary metabolite present in the extract. The microcapsules of extract-loaded chitosan were prepared using the ionic gelation method and characterized in terms of size, encapsulation efficiency (EE), and morphology of microcapsules. Fourier transform infrared (FTIR) was used to observe the successful production of microcapsules with a principal component analysis (PCA) approach. The antioxidant activity of microcapsules was established using the radical scavenging method. According to RSM, the highest amounts of TPC and TFC were obtained at 72.894 % ethanol, 2.031 h, and 57.384 °C. The compounds were employed from the optimized extract of *P. oleraceae* including phenolics and flavonoids. The microcapsules were secured with a %EE of $43.56 \pm 2.31$ %. The characteristics of microcapsules were approved for the obtained product's successful synthesis according to the PCA. The microcapsules have antioxidant activity in a concentration-dependent manner ($p < 0.0001$). The findings of this study underscored the benefits of employing chitosan as a nanocarrier for extract, offering a promising approach to enhance plant-derived therapies.

---

* Corresponding author.
  *E-mail address:* lokotdonna.lubis@usu.ac.id (L.D. Lubis).

## 1. Introduction

Currently, the use of extracts in disease treatment and prevention has increased rapidly [1]. This can be seen from the large number of studies that use extracts as subjects for more in-depth exploration regarding their function in health [2]. Several studies reported that extracts have properties and health benefits because they contain secondary metabolite compounds that have certain activities on the physiology of living things [3]. The increase in pharmacological activity will be directly influenced by the large content of secondary metabolites in the extracts tested and the response of the body of living creatures in processing these secondary metabolite compounds. Therefore, these factors must be considered by researchers in developing extracts as traditional medicines to provide the expected pharmacological effects [4–6].

Indonesia is one of the countries that uses many medicinal plants for the treatment and prevention of disease [7]. This is supported by various factors, including the Indonesian people's long-standing habit of using natural medicines and the abundant natural resources in Indonesia [8]. It is reported that *Portulaca oleraceae* is a medicinal plant that is often used traditionally to treat and prevent various diseases [9]. This herb is highly abundant in vital nutrients, primarily minerals, vitamins A, C, E, and B, and omega-3 fatty acids. It also includes bioactive phytochemicals like carotenoids and phenolic antioxidants, scientifically proven to provide significant health advantages [10]. This herb exhibits many activities, including antioxidant [11], anti-inflammatory [12], anticancer [13], antidiabetic [14], hepatoprotective [15], analgesic [16], skeletal muscle-relaxant [17], gastroprotective [18], neuroprotective [19], wound-healing [20], and antibacterial properties [21]. However, the effect is considered not optimal and can still be optimized through various methods such as optimizing the polyphenol content in the extract and increasing its bioavailability.

The positive effects mostly arise from the presence of polyphenols, such as flavonoids (particularly quercetin and kaempferol glycosides), phenolic acids, and proanthocyanidins [22]. It has been reported that increasing the amount of polyphenols in the extract will have a positive influence on the biological activity of the extract [23–27]. To obtain the optimal amount of polyphenols in the extract, several approaches need to be taken, such as choosing the right extraction method and monitoring extraction factors [28]. It has been reported that the extraction method has a significant influence on the withdrawal of active plant compounds. This is followed by the influence of factors in the process of producing optimal polyphenol levels [29]. One method that is often used to produce extracts with high amounts of polyphenols is reflux. Reflux is an extraction method at a certain temperature to speed up the extraction process and increase extraction efficiency [30,31]. However, time, temperature, and solvent used will have their influence and interact with each other. Therefore, efforts are needed to determine the best conditions in the extraction process that can produce extracts with optimum polyphenol levels using the Response Surface Methodology (RSM) [32].

Response Surface Methodology (RSM) is a combined method of mathematical and statistical approaches that can predict the best conditions of a process to produce products with certain conditions [33]. This response will illustrate how each variable influences the polyphenol content of the extract and the interaction effect of these factors [34]. The results of the analysis will describe the best conditions for producing extracts that have optimum polyphenolic compounds [35]. In this study, polyphenolic compounds will be described by the total phenol content and total flavonoid content of the extract as gallic acid equivalents and quercetin equivalents. As stated above, the amount of secondary metabolite compounds in an extract is not the only thing that influences the biological activity of the extract. The interaction of the extract with the body is another important factor for assessing the biological effectiveness of the extract [30]. The primary hindrance to the ineffective usage of these essential properties is the propensity of polyphenols to deteriorate during storage under varying temperatures, humidity levels, light exposure, and pH conditions [36]. In addition to their limited ability to be absorbed in the gastrointestinal tract, these substances also have low release from the food matrix, are unstable during digestion, and have limited diffusion across cell membranes. Therefore, microencapsulation was intended to safeguard these constituents [37].

The utilization of various techniques for microencapsulation has emerged as a viable solution to address the above limitations and enable the incorporation of polyphenols into diverse functional products [38]. The spray-drying process has been a widely used method for many years to encapsulate natural materials due to its cost-effectiveness and the abundance of equipment accessible for this purpose [39]. The process involves the conversion of a liquid substance into powder form through the utilization of carrier agent ingredients [40]. Chitosan, a chitin derivative that has undergone partial deacetylation and is made up of N-acetylglucosamine, has gained recognition as a noteworthy biomaterial and pharmaceutical excipient for delivering drugs [41]. This is due to its capacity to interact well with living organisms, break down naturally, provoke minimal immune response, and be obtained at a reasonable price [42]. Furthermore, its pharmaceutical applications are enhanced by its moderate toxicity as well as its hemostatic and bacteriostatic abilities [43]. This research focuses on developing microencapsulates from chitosan and polyphenol-rich extracts from *P. oleraceae* which will be reflected in the percentage of encapsulate efficiency. In addition, the resulting microencapsulates will be tested for their antioxidant activity, thereby increasing confidence in the resulting microencapsulates.

## 2. Materials and methods

### 2.1. Materials

The following chemicals were supplied by Sigma-Aldrich Corporation (St. Louis, MO, USA): chitosan extracted from shrimp shells, sodium tripolyphosphate, methyl alcohol, ethyl alcohol, glacial acetic acid, DPPH (2,2-diphenyl-1-picryhydrazyl), Folin-ciocalteu, aluminum chloride, gallic acid (3,4,5-trihydroxybenzoic acid), sodium citrate, and quercetin (3,3′,4',5,6-pentahydroxyflavone). All of these compounds were of the utmost purity grade.

## 2.2. Sample preparation and extraction

The *P. oleraceae* was collected from Sidodadi Regency, North Sumatera, Indonesia. The plant was found at 98°48′1.548″ East longitude and 3°38′36.225″ North latitude. The plant was identified as *P. oleraceae* by Medanese Herbarium, Faculty of Mathematics and Natural Sciences, Universitas Sumatera Utara Indonesia (Voucher Number: 305/UN5.2.1.1.2.4/Hmed/2023). The entire plant excluding a root was dried at 50 °C for 48 h. Approximately 500 g of the final dry matter content was ground into a fine powder and stored in a vacuum bag for preservation.

The extraction process was carried out using conventional reflux. All factors in extraction were prepared based on the results of Design-Expert V.13. Three factors were conducted for this extraction including extraction time ($X_1$), temperature ($X_2$), and solvent concentration ($X_3$). Seventeen experimental from three factors combinations were obtained for the extraction process [44]. Briefly, 20 g dry powder of *P. oleraceae* was soaked with 200 mL solvents in the bottom round flask. The extraction conditions were followed in Table 1. After the extraction process for each condition, the crude extract was filtrated with filter paper (4–12 μm). All collected samples were placed into a glass flask and concentrated using a rotary evaporator vacuum with slow speed at 110 rpm, at 65 °C, for about 3 h.

## 2.3. Determination of total phenolic and flavonoid contents

The crude extract's total phenolic content (TPC) was measured using a spectrophotometric method that has been previously published. In summary, a total of 100 μL of extract (used as a solvent for the blank), 200 μL of Folin–Ciocalteu reagent, 2 mL of distilled water, and 1 mL of $Na_2CO_3$ were combined in a reaction tube. The mixture was then incubated at a temperature of 50 °C for 25 min. Subsequently, the absorbance of the mixture was measured at a wavelength of 765 nm using a VWR UV-1600PC Spectrophotometer (VWR, Wayne, PA, USA), with gallic acid serving as the standard. The samples were subjected to triplicate analysis, and the total phenolic content (TPC) was quantified as the average value of gallic acid equivalents (GAE) in milligrams per gram of sample, with the standard deviation indicated [45].

In addition, the calorimetric method was employed to determine the total flavonoid content in the samples, building upon prior research. Quercetin was employed to establish standard calibration curves for the quantification of flavonoids. The samples were dissolved in 5 mL of distilled water and subjected to incubation at a temperature of 40 °C for 45 min. Subsequently, the samples were centrifuged at a speed of 1000 rpm for 10 min 1.2 mL of the produced solution was combined with an equal volume of 2 % aluminium chloride, resulting in a total volume of 2.4 mL. Following the mixing process, the solution was left to incubate for 60 min at room temperature. The solution's absorbance was quantified at a wavelength of 420 nm. The overall concentration of flavonoid content in the test sample was determined by analyzing the quercetin standard curve plot and reported as milligrams of quercetin equivalent (QE) per gram [45].

## 2.4. Conception of experiment and statistical analysis

This experiment was carried out utilizing independent variables, specifically $X_1$, $X_2$, and $X_3$, each set at three different levels. The experimental design employed for this purpose was the BBD. The comprehensive design comprised a total of 17 experimental points. The encodings and actual values of the experimental design components are shown in Table 1.

Multiple regression analysis was applied to the BBD's experimental data to find a good fit with the second-order polynomial model, as shown below (Eq. (1)).

**Table 1**
Box-Behnken design (BBD) for independent variables and corresponding response values (experimental).

| Run | Independent variables | | | Responses | |
|-----|-----------------------|--------------|-------------|-------------------------|----------------------|
|     | $X_1$ (%)             | $X_2$ (°C)   | $X_3$ (hours) | TPC (mg GAE/ g sample) | TFC (mg QE/ g sample) |
| 1   | 90 | 60 | 1 | 6.90 ± 0.21 | 20.97 ± 0.92 |
| 2   | 90 | 50 | 2 | 7.32 ± 0.28 | 21.57 ± 0.85 |
| 3   | 70 | 60 | 2 | 9.52 ± 0.35 | 26.95 ± 0.95 |
| 4   | 70 | 60 | 2 | 9.01 ± 0.31 | 28.01 ± 0.79 |
| 5   | 90 | 70 | 2 | 5.12 ± 0.15 | 19.96 ± 0.63 |
| 6   | 90 | 60 | 3 | 5.82 ± 0.14 | 18.36 ± 0.92 |
| 7   | 70 | 70 | 3 | 6.72 ± 0.27 | 25.91 ± 1.13 |
| 8   | 50 | 50 | 2 | 4.78 ± 0.12 | 17.03 ± 0.82 |
| 9   | 50 | 60 | 1 | 3.20 ± 0.09 | 17.73 ± 0.87 |
| 10  | 70 | 60 | 2 | 8.78 ± 0.30 | 27.21 ± 1.67 |
| 11  | 50 | 70 | 2 | 2.97 ± 0.08 | 24.72 ± 1.21 |
| 12  | 70 | 60 | 2 | 8.90 ± 0.31 | 27.35 ± 1.07 |
| 13  | 50 | 60 | 3 | 3.98 ± 0.09 | 17.95 ± 0.82 |
| 14  | 70 | 50 | 1 | 5.82 ± 0.15 | 26.31 ± 1.08 |
| 15  | 70 | 50 | 3 | 7.95 ± 0.40 | 25.31 ± 1.10 |
| 16  | 70 | 60 | 2 | 8.58 ± 0.43 | 28.62 ± 0.97 |
| 17  | 70 | 70 | 1 | 4.14 ± 0.11 | 23.85 ± 0.90 |

$$Y = Z_0 \sum_{i=1}^{3} Z_i + \sum_{i=1}^{3} Z_{ii} X_i^2 + \sum_{j=i+1}^{3} Z_{ij} X_i X_j \tag{1}$$

in the given equation, Y is the response function which comprises TPC ($Y_1$) and TFC ($Y_2$). $Z_0$ is a constant term, while $Z_i$, $Z_{ii}$, and $Z_{ij}$ indicate the coefficients of the linear, quadratic, and interaction factors, respectively. $X_i$ and $X_j$ are the independent variables in the equation [46]. An analysis of variance (ANOVA) was conducted to assess the lack of fit, determination coefficient ($R^2$), and the impact of linear, quadratic, and interaction terms on each response variable. The RSM was employed to construct three-dimensional charts representing the response surface. The experimental design, analysis of experimental data, model fitting, and optimization procedure were conducted using Design Expert V. 13 Software. To assess the distinction between the mean and the predicted value and observation value (by a one-sample *t*-test), as well as the Pearson correlation, the statistical software IBM SPSS Statistics (IBM Co., Ltd., America, United States) was employed [46].

## 2.5. Phytochemical analysis of polyphenol-rich extract

The analysis was conducted via liquid chromatography with the Thermo Scientific™ Vanquish™ UHPLC Binary Pump, coupled with Orbitrap high-resolution mass spectrometry using the Thermo Scientific™ Q Exactive™ Hybrid Quadrupole-Orbitrap™ High-Resolution Mass Spectrometer. The liquid chromatography analysis was conducted using a Thermo Scientific™ Accucore™ Phenyl-Hexyl analytical column with dimensions of 100 mm length, 2.1 mm inner diameter, and 2.6 μm particle size. The mobile phases

**Table 2**
ANOVA for quadratic model.

| ANOVA for quadratic model for TPC | | | | | | | |
|---|---|---|---|---|---|---|---|
| Source | RC | SS | DF | MS | F-value | *p*-value | |
| Model | | 70.81 | 9 | 7.87 | 14.21 | 0.0010 | Significant |
| Intercept | 8.96 | | | | | | |
| Linear terms | | | | | | | |
| $X_1$ | 1.28 | 13.08 | 1 | 13.08 | 23.63 | 0.0018 | Significant |
| $X_2$ | −0.8650 | 5.99 | 1 | 5.99 | 10.81 | 0.0133 | Significant |
| $X_3$ | 0.5513 | 2.43 | 1 | 2.43 | 4.39 | 0.0744 | Not significant |
| Interaction terms | | | | | | | |
| $X_1 X_2$ | −0.0975 | 0.0380 | 1 | 0.0380 | 0.0687 | 0.8008 | Not significant |
| $X_1 X_3$ | −0.4650 | 0.8649 | 1 | 0.8649 | 1.56 | 0.2515 | Not significant |
| $X_2 X_3$ | 0.1125 | 0.0506 | 1 | 0.0506 | 0.0914 | 0.7711 | Not significant |
| Quadratic terms | | | | | | | |
| $X_1^2$ | −2.55 | 27.30 | 1 | 27.30 | 49.32 | 0.0002 | Significant |
| $X_2^2$ | −1.36 | 7.83 | 1 | 7.83 | 14.15 | 0.0071 | Significant |
| $X_3^2$ | −1.44 | 8.69 | 1 | 8.69 | 15.69 | 0.0055 | Significant |
| Lack of fit | | 3.38 | 3 | 1.13 | 9.07 | 0.0694 | Not significant |
| Pure error | | 0.4965 | 4 | 0.1241 | | | |
| $R^2$ | | | | | | 0.9481 | |
| Adjusted $R^2$ | | | | | | 0.8814 | |
| Adeq precision | | | | | | 11.0009 | |
| C.V.% | | | | | | 11.55 | |
| ANOVA for quadratic model for TFC | | | | | | | |
| Source | RC | SS | DF | MS | F-value | *p*-value | |
| Model | | 247.42 | 9 | 27.49 | 14.71 | 0.0009 | Significant |
| Intercept | 8.96 | | | | | | |
| Linear terms | | | | | | | |
| $X_1$ | 1.28 | 1.47 | 1 | 1.47 | 0.7869 | 0.4045 | Not significant |
| $X_2$ | −0.8650 | 2.23 | 1 | 2.23 | 1.19 | 0.3112 | Not significant |
| $X_3$ | 0.5513 | 0.2211 | 1 | 0.2211 | 0.1183 | 0.7410 | Not significant |
| Interaction terms | | | | | | | |
| $X_1 X_2$ | −0.0975 | 21.62 | 1 | 21.62 | 11.57 | 0.0114 | Significant |
| $X_1 X_3$ | −0.4650 | 2.00 | 1 | 2.00 | 1.07 | 0.3351 | Not significant |
| $X_2 X_3$ | 0.1125 | 2.34 | 1 | 2.34 | 1.25 | 0.3000 | Not significant |
| Quadratic terms | | | | | | | |
| $X_1^2$ | −2.55 | 189.02 | 1 | 189.02 | 101.14 | <0.0001 | Significant |
| $X_2^2$ | −1.36 | 0.0489 | 1 | 0.0489 | 0.0262 | 0.8761 | Not significant |
| $X_3^2$ | −1.44 | 19.92 | 1 | 19.92 | 10.66 | 0.0138 | Significant |
| Lack of fit | | 11.24 | 3 | 3.75 | 8.14 | 0.0754 | Not significant |
| Pure error | | 1.84 | 4 | 0.4604 | | | |
| $R^2$ | | | | | | 0.9498 | |
| Adjusted $R^2$ | | | | | | 0.8852 | |
| Adeq precision | | | | | | 9.6226 | |
| C.V.% | | | | | | 5.84 | |

employed in the experiment were MS-grade water with 0.1 % formic acid (A) and MS-grade methanol with 0.1 % formic acid (B). The experiment utilized a gradient approach with a flow rate of 0.3 mL/min. Initially, the mobile phase B was adjusted to a concentration of 5 % and then systematically raised to 90 % over a period of 16 min. Subsequently, it remained at a steady level of 90 % for a duration of 4 min, and then returned to the original state of 5 % B until 25 min had elapsed. The temperature of the column was adjusted to 40 °C, and the volume of the injection was 3 μL. The unspecific screening was conducted using complete MS/dd-MS2 acquisition mode in positive polarity [47].

### 2.6. Formulation and characterization of microencapsulate

#### 2.6.1. Microencapsulate synthesis using ionic gelation method

The polyphenol-rich extract was encapsulated using the ionic gelation method in combination with sodium tripolyphosphate, following the approach outlined by Vonghirundecha et al. (2022) [48] with minor adjustments. In summary, the wall-material components of chitosan at a concentration of 0.1 % (w/v) were dissolved in a solution of 1 % (v/v) acetic acid and blended with sodium tripolyphosphate at a concentration of 2 % (w/v). The mixture was then agitated at a temperature of 65 °C until it became uniform. The process of encapsulation was accomplished by incorporating the polyphenol-rich extract into the wall material at a ratio of 1:1 (v/v) while continuously stirring at room temperature for the duration of one night.

#### 2.6.2. Particle size and morphological analysis

The microcapsules of *P. oleraceae* extract with chitosan were analyzed for particle size using the CORDOUAN Technologies Particle Size Analyzer at room temperature [49]. Additionally, the surface morphology and structure of the microcapsules were analyzed using a scanning electron microscope (SEM) model TM 3000 Hitachi. The examination was conducted at magnifications 2500 × to
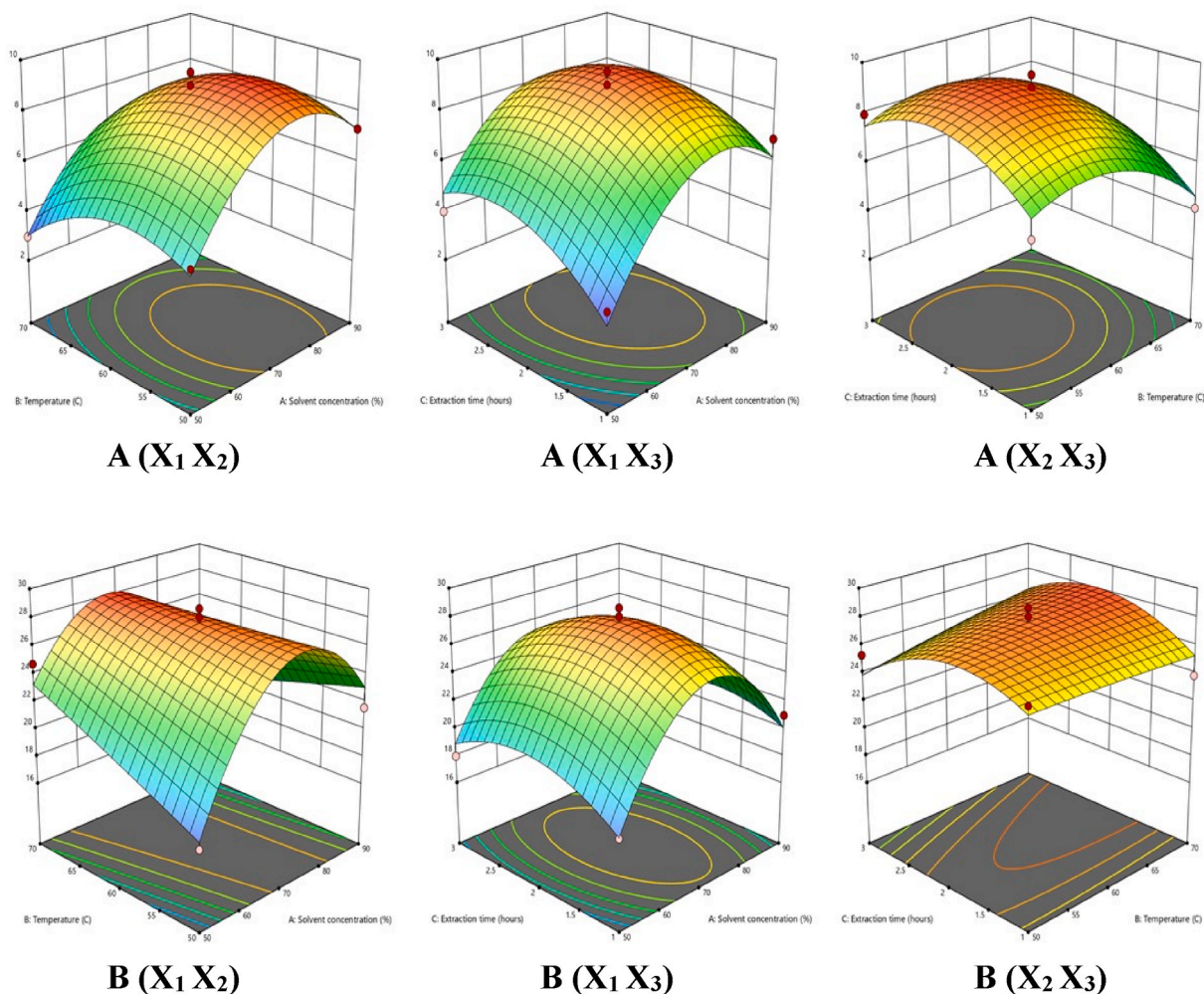


**Fig. 1.** The three-dimensional (3D) response surface plots of *P. oleraceae* extraction for TPC (A) and TFC (B) for solvent concentration, temperature, and extraction time as a function of key interaction factors for RSM.

accurately identify the particles' morphology [50].

### 2.6.3. Fourier-transform infrared (FT-IR) and principle component analysis

Chitosan powder, extract, and microcapsules were subjected to Fourier Transform Infra-Red (FT-IR) analysis using KBr pellets. The analysis was conducted in the region of 500–4000 cm$^{-1}$ using a Shimadzu instrument. Following the measurements, a graph depicting the percentage of light transmission in relation to the wavelength was created for each sample. The distinctive peak corresponding to the chemical bond was identified [51]. The samples' FTIR spectra were subsequently analyzed using principal component analysis (PCA) in Minitab v.16 software (Minitab Inc., State College, PA). PCA operates by transforming the spectrum of an n-dimensional variable (spectra) into a PC, where each spectrum in the dataset is represented by a single score in a lower-dimensional space. The PCA are arranged in order of their eigenvalues, which measure the extent to which each PC captures variance. Subsequently, the PCA exhibiting the highest eigenvalues, which correspond to the most substantial changes in the FTIR spectra, are selected and preserved. Conversely, the PCA that solely encompass noise are rejected, since they possess the lowest eigenvalues. PCA score plots were employed to objectively classify samples based on their measured attributes [52].
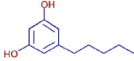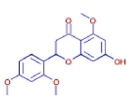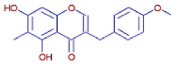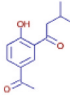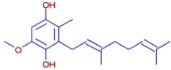
### 2.6.4. Encapsulation efficiency

The encapsulation efficiency (EE) is the proportion of active chemicals that are enclosed within the polymer solution, represented as a percentage. The efficiency of shielding materials in trapping the extract is shown by this value. The calculation of the encapsulation efficiency was performed using Eq. (2) [53].

$$\% \, EE = \frac{Total \; Phenolic \; Content \; in \; Microencapsulate}{Total \; Phenolic \; Content \; in \; Extracts} \; x \; 100\% \tag{2}$$

**Table 3**
The evaluation of phenolic and flavonoid compounds using LC-HRMS.

| Plant secondary metabolite | Chemical formula | m/z (M + H$^+$) | Retention time (min) | Chemical structure |
|---|---|---|---|---|
| *Trans*-p-Coumaraldehyde | $C_9 H_8 O_2$ | 149.05960 | 1.445 | |
| 5-Pentylresorcinol | $C_{11} H_{16} O_2$ | 181.12209 | 9.250 | |
| (3R,4R)-4-(3,4-Dihydroxybenzyl)-3-(3-hydroxy benzyl)dihydro-2(3H)-furanone | $C_{18} H_{18} O_5$ | 315.12219 | 10.207 | |
| 2-(2,4-Dimethoxyphenyl)-7-hydroxy-5-methoxy-2,3-dihydro-4H-chromen-4-one | $C_{18} H_{18} O_6$ | 331.11710 | 10.910 | |
| 4-Vinylcatechol | $C_8 H_8 O_2$ | 137.05966 | 0.806 | |
| Ophiopogonone B | $C_{18} H_{16} O_5$ | 313.10651 | 10.109 | |
| 1-(5-Acetyl-2-hydroxyphenyl)- 3-methyl-1-butanone | $C_{13} H_{16} O_3$ | 223.13261 | 5.913 | |
| 3-[(2E)-3,7-Dimethyl-2,6-octadien-1-yl]-5-methoxy-2-methyl-1,4-benzenediol | $C_{18} H_{26} O_3$ | 331.28378 | 15.085 | |
| m-Cresol | $C_7 H_8 O$ | 194.15388 | 7.974 | |

## 2.7. Antioxidant activity of microencapsulate using the DPPH method

The antioxidant activity of extract and microcapsules can be assessed by their ability to scavenge DPPH. The samples were generated at different concentrations, specifically 15.625, 31.25, 62.5, 125.00, 250.00, and 500.00 μg/mL. Subsequently, 100 μL of each sample were combined with 125 μL of DPPH methanolic solution and allowed to react at room temperature for a duration of 30 min. The spectrophotometric measurement of absorbance at 517 nm was conducted using a UVmini-1240 spectrophotometer (Shimadzu, Japan), with a blank sample as the reference. The trials were conducted three times in order to ensure accuracy, with ascorbic acid being utilized as a reference for comparison. The calculation of the free radical scavenging activity was performed using Eq. (3) [54].

$$\% \textbf{\textit{Radical Scavenging Activity}} = \frac{\textbf{\textit{Abs control}} - \textbf{\textit{Abs sample}}}{\textbf{\textit{Abs control}}} \textbf{\textit{x}} \ \textbf{100}\% \tag{3}$$
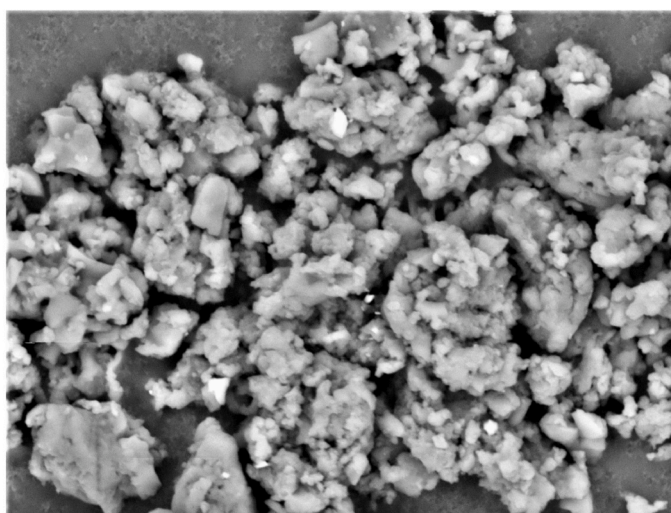
## 3. Results and discussion

### 3.1. Fitting of the RSM

Table 1 describes the experimental conditions and conclusions for each extraction condition. All response variables were converted

**A**
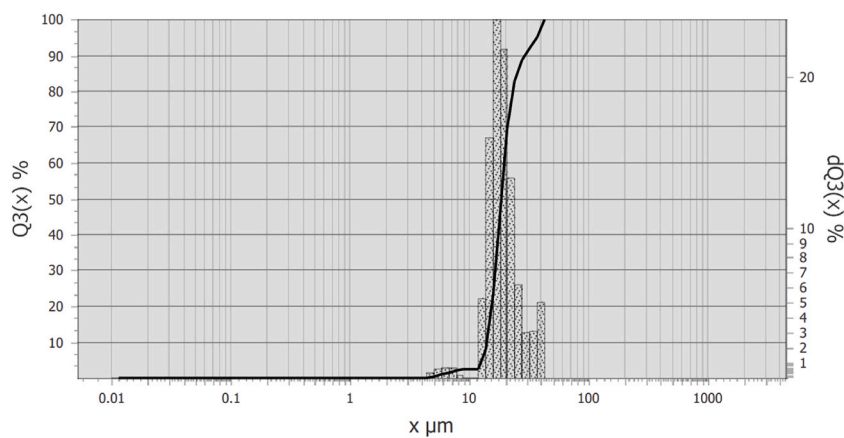
**B**

**Fig. 2.** The characteristic of *P. oleraceae* extract-chitosan microcapsule. Particle size analysis (A) and Morphological analysis using SEM with a magnification of 2500 (B).

into second-order quadratic polynomial equations to accommodate variations in answers based on extraction factors. The statistical significance of the fitted second-order quadratic model equations was assessed using ANOVA. The regression coefficient (β), the adjusted correlation coefficient ($R^2$), coefficient of variation (CV), and sufficient precision were employed to quantify the degree of fit of the model (Table 2). The terms with p-values greater than 0.05 were removed from the models to enhance the accuracy and predictive power. The *p*-values were utilized to determine the significance of each coefficient. When the *p*-values were less than 0.05, 0.01, and 0.001, the model terms were statistically significant, very significant, and extremely significant, respectively.

Table 2 demonstrates that the model terms have a substantial impact, with a *p*-value of less than 0.001. The $R^2$ values of the constructed regression models exceed 0.94, indicating a substantial degree of statistical significance. An optimal signal-to-noise ratio is indicated by a suitable level of precision, with a value greater than 4 being considered desirable according to Choi et al. (2022) [55]. The Adeq accuracy ratio for TPC and TFC is 11.00 and 9.62, respectively, indicating a strong signal and appropriateness for this approach. The CV quantifies the degree of consistency in a model, with TPC and TFC yielding values of 11.55 and 5.48, respectively. These values suggest that the model is highly replicable. Three-dimensional surfaces and contour plots were generated using several linear regression equations to illustrate the interactions between independent variables (Fig. 1. A and B).

### 3.2. Influence of variables on TPC and TFC

The TPC and TFC were determined for 17 extracts according to the experimental design outlined in Table 1. The extracts included TPC and TFC in the range of $2.97 \pm 0.25$ to $9.52 \pm 0.35$ mg GAE/g and $17.03 \pm 0.64$ to $28.62 \pm 0.74$ mg QE/g, respectively. The equations presented in Eqs. (4) and (5) are second-order polynomials that demonstrate the connections between TPC, TFC, and their respective variables.

$$Y\ TPC\ (mg\ GAE/g) = 8.96 + 1.28 \times X_1 - 0.8650 \times X_2 + 0.5513 \times X_3 - 0.0975 \times X_1 \times X_2 - 0.4650 \times X_1 \times X_3 + 0.1125 \times X_2 \times X_3 - 2.55 \times X_1^2 - 1.36 \times X_2^2 - 1.44 \times X_3^2 \tag{4}$$

$$Y\ TFC\ (mg\ QE/g) = 27.63 + 0.4287 \times X_1 + 0.5275 \times X_2 - 0.1663 \times X_3 - 2.32 \times X_1 \times X_2 - 0.7075 \times X_1 \times X_3 + 0.7650 \times X_2 \times X_3 - 6.71 \times X_1^2 - 0.1078 \times X_2^2 - 2.18 \times X_3^2 \tag{5}$$

The lack of fit values for TPC and TFC were not statistically significant ($p = 0.0694$ and 0.0754, respectively), indicating that the model successfully predicted $R^2$ values of 0.9481 (TPC) and 0.9498 (TFC), as well as Adj. $R^2$ values of 0.8814 (TPC) and 0.8852 (TFC) (Table 2). The RSM model precisely forecasted the effects of the parameters on the TPC and TFC of the extract. According to Fig. 1 A and B, the combination of 70 % ethanol and a temperature of 60 °C resulted in the highest TPC and TFC after 2 h. Sedraoui et al., found that medium-concentration ethanol increases the polarity of the solvent, resulting in the dissolution of phenolic compounds that are polar or moderately polar [56]. The presence of a moderate amount of ethanol in water can have an impact on the arrangement and composition of phospholipids in cell membranes. This phenomenon impacts the permeability of plant cells, resulting in increased extraction and diffusion of polyphenols [57]. The previous comparative study conducted experiments that revealed that the extraction of phenolic compounds from green tea leaves was enhanced by high hydrostatic pressure when ethanol was present in the solvent. The extraction reached its maximum efficiency at a concentration of 50 % ethanol and decreased thereafter [58].

### 3.3. Model validation

The desirability function concurrently optimizes TPC and TFC. The desirability function was employed to predict the parameters, enabling a multivariate analysis to determine the optimal value for all responses in a single extraction [59]. The study utilized the
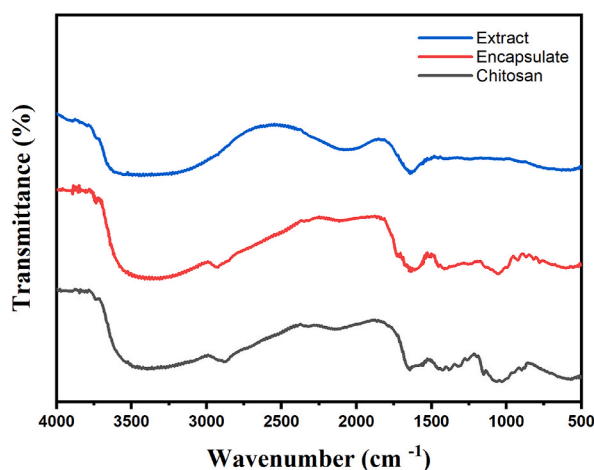


**Fig. 3.** The FTIR spectrum of *P. oleraceae* extract, microcapsules, and chitosan in a wavenumber of 4000–500 cm$^{-1}$..

**Table 4**
Assignment of the FTIR spectra.

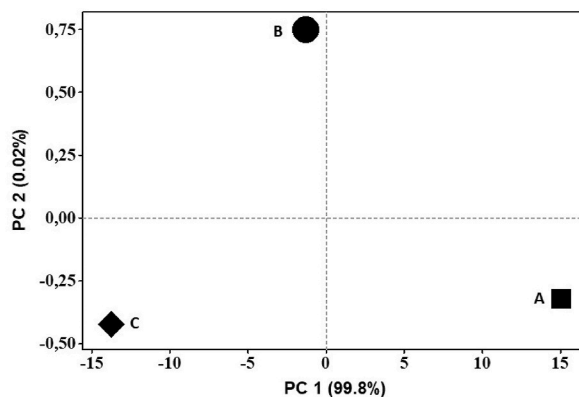| No | P. oleraceae Extract | | Microcapsules | |
|---|---|---|---|---|
| | Wavenumber (cm$^{-1}$) | Functional groups | Wavenumber (cm$^{-1}$) | Functional groups |
| 1 | 3471.87 | O–H stretch | 3394.72 | O–H stretch |
| 2 | 1515.12 | C=C stretch | 2926.01 | C–H stretch |
| 3 | 1417.68 | C–C stretch | 1257.57 | N–H stretch |
| 4 | 1020.34 | C–O–C stretch | 1055.06 | P=O stretch |

following conditions: $X_1$ at 72.894 %, $X_2$ at 57.384 °C, and $X_3$ at 2.031 h, to attain the highest possible overall attractiveness, which was measured at D = 0.929. Given the ideal conditions, the expected values for TPC and TFC are 9.23 mg GAE/g and 27.476 mg QE/g, respectively. In order to establish the adequacy of the model equations, a replicated experiment was carried out in the optimal conditions projected by Derringer's desire model. The obtained results are as follows: TPC is 10.97 ± 0.74 mg GAE/g and TFC is 29.86 ± 0.94 mg QE/g. The model effectively optimized the shared extraction parameters for all answers, as demonstrated by the strong correspondence between experimental and anticipated values. The identification of phenolic and flavonoid components in the extract was conducted using liquid chromatography-orbitrap high-resolution mass spectrometry (LC-Orbitrap HRMS). Table 3 demonstrates the identification of 9 compounds as phenolic and flavonoid in positive mode using comprehensive MS/dd-MS2 acquisition data. This data includes the precursor ion mass, fragments, recognized fragmentation patterns specific to the compounds, neutral mass loss, and information obtained from literature and online databases.

### 3.4. Characteristics and morphology of extract-chitosan microencapsulate

The ionic gelation process was utilized to create a microencapsulated extract of *P. oleraceae*. The synthesis of microcapsules containing *P. oleraceae* extract was successfully achieved by using pH 4, 90 min of stirring time, and 0.1 % (w/v) chitosan. The percentage of encapsulation efficiency (%EE) is reported as 43.56 ± 2.31 %. The amino group in chitosan can undergo protonation in an acidic environment, resulting in a neutral solution. This protonation process is influenced by the pKa value of the amino group, which is approximately 6.5 [60]. Despite the protonation of the amino group in an acidic solution, it is possible to enhance the solubility of chitosan [61]. The utilization of this characteristic holds significant significance in biological applications, particularly when chitosan is employed for drug delivery to sites in acidic environments [62]. At a pH of 4, chitosan attracts a greater number of proton donors, leading to the protonation of more amine groups ($NH_2$) into $NH^{+3}$ ions. These ions then form ionic cross-links with NaTPP, resulting in the formation of microcapsules [63]. The abundance of protonated chitosan will enhance chitosan's capacity to absorb the bioactive chemicals from the extract, hence augmenting the encapsulation efficiency [64].

This observation closely resembled a prior study by Khorshidian et al. [65], which showed that pH 4 was the optimal pH for formulating microcapsules containing chitosan. The charge densities of biopolymers with opposite signs were stoichiometrically balanced at a pH of 4. If the pH was below the optimal level, the degree of ionization of amine groups on the chitosan molecular chain hindered the creation of uniform particles in the solution [66]. At pH values over 4, the degree of ionization and solubility of chitosan reduced, likely leading to variability in size distribution [67].

The microcapsules that were obtained were then described based on their dimensions and surface morphology. An examination of the size distribution of particles can provide valuable insights into the behavior of microcapsules and assist in predicting their stability



**Fig. 4.** The distribution of samples based on % transmittance in the wavenumber of fingerprint area. Chitosan (A), *P. oleraceae* extract (B), and Microcapsules (C).
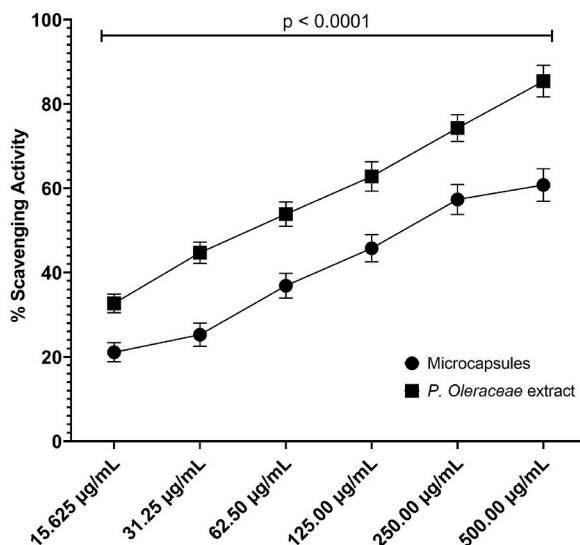
**Fig. 5.** The antioxidant activity of *P. oleracea* extract and microcapsules against DPPH radical in a variation of concentrations. The result showed significant differences between extract and microcapsules using a *t*-test with $p < 0.0001$.

[68]. The average size of the particles, as seen in Fig. 2A, was $19.89 \pm 0.76$ μm and Fig. 2B displays the SEM picture. Concerning the SEM images (Fig. 2B), the microcapsules exhibit a greater abundance of spherical and uniform forms. Nevertheless, the outside of the microcapsules exhibited some degree of unevenness [69]. However, the study did not evaluate the viscosity of the microcapsules, which is a shortcoming.

The sizes and surfaces of the microcapsules containing *P. oleraceae* extract seem to be comparable to those of the typical microcapsules. Other authors have also achieved comparable outcomes using the ionic gelation approach, producing microcapsules that are tiny, spherical, and exhibit some imperfections and roughness [70,71]. However, the microcapsule product already fell into the range of microcapsule sizes, with an average diameter of $19.89 \pm 0.76$ μm.

The FTIR analysis was performed to further investigate the microcapsules. Fig. 3., presents the FTIR findings, and the identification of the significant peaks is listed in Table 4. The prominent peaks of the bioactive compounds in *P. oleraceae* were found at specific wavenumbers: 3471.87 cm$^{-1}$ (corresponding to O–H stretching), 1515.12 cm$^{-1}$ (corresponding to C═C stretching), 1417.68 cm$^{-1}$ (corresponding to C–C stretching), and 1020.34 cm$^{-1}$ (corresponding to C–O–C stretching) (Fig. 3) [72]. A subset of these peaks were detected within microcapsules. The FTIR spectra of the microcapsules exhibit a displacement in the O–H functional group at the encapsulate peak. Initially, the peak was observed at a wavenumber of 3471.87 cm$^{-1}$ and subsequently relocated to 3394.72 cm$^{-1}$. The detection of a novel absorption peak at 2926.01 cm$^{-1}$ and 1257.57 cm$^{-1}$ indicates the existence of a stretching motion of C–H bonds in an alkane and the presence of a N–H group from an amine. This small peak is attributed to chitosan, which was employed as a covering material for the microcapsules [73]. The presence of a phosphate group (P═O) is indicated by the absorption peak observed at 1055.06 cm$^{-1}$. This suggests that the peak originated from NaTPP, which was used as a crosslinker during the manufacture of microcapsules [74].

FTIR measurement indicates that chitosan microcapsules effectively incorporated bioactive compounds from the extracts through ionic crosslinking using the microprecipitation method. The detection of distinctive peaks corresponding to bioactive molecules (1514.12 cm$^{-1}$ for C═C aromatics) on the microcapsules serves as conclusive proof that the bioactive molecules were effectively crosslinked to the chitosan microcapsules [72]. In addition, the microcapsule exhibited distinct peaks at 1257.57 cm$^{-1}$ for N–H amines and 1055.06 cm$^{-1}$ for P═O, but these peaks were not present in the extract [74]. This outcome is corroborated by the PCA data obtained from the extraction process, microcapsules, and chitosan.

The PCA was used to ensure further differentiation of microcapsules based on the FTIR transmittance of each sample. Fig. 4 shows the PCA score plot using two principal components accounting for 100 % of the total variance with PC1 and PC2, explaining 99.8 % and 0.02 % of the total variance, respectively. Based on the score plot, all samples were clustered into their respective groups. This plot clarifies the similarities and differences in the FTIR spectrum of the microcapsule; the closer one group is to another, the greater the similarity in the composition of each sample [75]. It shows that the microcapsule is separated from the extract and chitosan. All data shows that the microcapsule of *P. oleraceae* extract and chitosan has succeeded in producing.

### 3.5. Antioxidant activity of microcapsule

The DPPH technique was employed to evaluate the antioxidant activity of both the microcapsule and extract. The outcomes are illustrated in Fig. 5. The microcapsule demonstrates activity in scavenging DPPH radicals that varies depending on their concentration. At a dose of 500.00 μg/mL, the microcapsules exhibited a significant ability to inhibit $60.75 \pm 3.85$ % of DPPH radicals. The activity

diminishes as the concentration drops from 250.00 μg/mL to 15.625 μg/mL. The activity decreases by $57.31 \pm 3.56$ %, $45.72 \pm 3.25$ %, $36.85 \pm 2.94$ %, $25.23 \pm 2.75$ %, and $21.07 \pm 2.25$ % respectively. The efficacy of microcapsules is significantly lower than that of extracts, having a *p*-value of less than 0.0001. The extract, administered at a concentration of 500.00 μg/mL, exhibited a notable capacity to suppress DPPH radicals by $85.36 \pm 3.75$ %. The inhibition found with microcapsules was significantly distinct from this ($p < 0.001$). The extract demonstrated increased activity at different concentrations, with values of $74.27 \pm 3.17$ %, $62.78 \pm 3.51$ %, $53.85 \pm 2.86$ %, $44.68 \pm 2.52$ %, and $32.68 \pm 2.21$ %, respectively ($p < 0.001$).

The results indicate that the microcapsules of *P. oleraceae* demonstrate diminished biological efficacy in comparison to the non-microencapsulated extract. The current study demonstrates a comparable outcome to the previous research, indicating that the antioxidant activity of microcapsules is inferior to that of the extract [76]. This phenomenon may occur due to the partial liberation of the bioactive substances enclosed in the microcapsules, leading to the retention of certain molecules within the microcapsules [77]. Furthermore, the main purpose of microencapsulation is not to increase biological activity, but rather to protect and control the release of active chemicals. Nevertheless, microcapsules containing extracts derived from *P. oleraceae* remain efficacious for utilization as antioxidants. The utilization of microcapsules containing the *P. oleraceae* extract exhibits potential as a natural antioxidant agent.

## 4. Conclusions

This study provides the optimization models to produce a polyphenol-rich extract of *P. oleraceae* using the RSM approach. The optimum condition was validated in $X_1$: 72.894 %, $X_2$: 57.384 °C: and $X_3$, 2.031 h. The experimental data showed TPC and TFC are not significantly different from the predicted data of $10.97 \pm 0.74$ mg GAE/g and $29.86 \pm 0.94$ mg QE/g, respectively. The microcapsules of the extract under optimum conditions were successfully produced using chitosan and NaTPP with a % EE of $43.56 \pm 2.31$ %. The FTIR measurement revealed the formation of cross-linking between chitosan and NaTPP. The scanning electron microscopy (SEM) examination revealed that the surface of the encapsulated extracts was characterized by a rough texture and predominantly spherical shape. However, the particle size analysis (PSA) demonstrated that the micro-sized particles were obtained with an average diameter of $19.89 \pm 0.76$ μm. The microcapsules retained the antioxidant properties but at a lesser level compared to the extract. This work facilitates the crucial role of microencapsulation in producing the polyphenol-rich extract of *P. oleraceae*.

## Funding

## Data availability

Data will be made available on request.

## CRediT authorship contribution statement

**Lokot Donna Lubis:** Supervision, Funding acquisition, Conceptualization. **Arya Tjipta Prananda:** Writing – original draft, Validation, Project administration. **Nur Aira Juwita:** Investigation, Funding acquisition, Conceptualization. **Muhammad Amin Nasution:** Writing – original draft, Funding acquisition, Conceptualization. **Rony Abdi Syahputra:** Writing – review & editing, Project administration, Investigation. **Sumaiyah Sumaiyah:** Software, Methodology, Investigation, Data curation. **Rodiah Rahmawaty Lubis:** Writing – review & editing, Supervision. **Muhammad Fauzan Lubis:** Writing – original draft, Software, Investigation, Funding acquisition, Conceptualization. **Ririn Astyka:** Validation, Resources, Project administration, Methodology. **Jihan Firyal Atiqah:** Software, Project administration, Data curation.

## Declaration of competing interest

The authors declare that they have no known competing financial interests or personal relationships that could have appeared to influence the work reported in this paper.

## Acknowledgments

## References

[1] M.F. Lubis, P.A.Z. Hasibuan, H. Syahputra, C. Surbakti, R. Astyka, *Sarauia vulcani* (Korth.) as herbal medicine potential from North Sumatera, Indonesia: a literature review, Heliyon 8 (4) (2022) e09249.

[2] A. Altemimi, N. Lakhssassi, A. Baharlouei, D.G. Watson, D.A. Lightfoot, Phytochemicals: extraction, isolation, and identification of bioactive compounds from plant extracts, Plants 6 (4) (2017) 42.

[3] R.A. Syahputra Adrian, N.A. Juwita, R. Astyka, M.F. Lubis, Andaliman (*Zanthoxylum acanthopodium* DC.) a herbal medicine from North Sumatera, Indonesia: phytochemical and pharmacological review, Heliyon 9 (5) (2023) e16159.

[4] B.M. Twaij, M.N. Hasan, Bioactive secondary metabolites from plant sources: types, synthesis, and their therapeutic uses, Int. J. Plant Biol. 13 (1) (2022) 4–14.

[5] S.G. Gandhi, V. Mahajan, Y.S. Bedi, Changing trends in biotechnology of secondary metabolism in medicinal and aromatic plants, Planta 241 (2) (2015) 303–317, 2015.

[6] M.F. Lubis, S. Sumaiyah, L.D. Lubis, K. Fitri, R. Astyka, Application of Box-Behnken design for optimization of *Vernonia amygdalina* stem bark extract in relation to its antioxidant and anti-colon cancer activity, Arab. J. Chem. (2024) 105702.

[7] F.H. Arifah, A.E. Nugroho, A. Rohman, W. Sujarwo, A review of medicinal plants for the treatment of diabetes mellitus: the case of Indonesia, South Afr. J. Bot. 149 (2022) 537–558.

[8] A.B. SuwardiMardudi, Z.I. NaviaBaihaqi, Muntaha, Documentation of medicinal plants used by Aneuk Jamee tribe in Kota Bahagia sub-district, South Aceh, Indonesia, Biodiversitas 22 (1) (2021) 6–15.

[9] M. Iranshahy, B. Javadi, M. Iranshahi, S.P. Jahanbakhsh, S. Mahyari, F.V. Hassani, G. Karimi, A review of traditional uses, phytochemistry and pharmacology of *Portulaca oleracea* L, J. Ethnopharmacol. 205 (2017) 158–172.

[10] K. Li, T. Xia, Y. Jiang, N. Wang, L. Lai, S. Xu, X. Yue, H. Xin, A review on ethnopharmacology, phytochemistry, pharmacology and potential uses of *Portulaca oleracea* L, J. Ethnopharmacol. 319 (Pt 2) (2024) 117211.

[11] MdK. Uddin, A.S. Juraimi, Md E. Ali, M.R. Ismail, Evaluation of antioxidant properties and mineral composition of purslane (*Portulaca oleracea* L.) at different growth stages, Int. J. Mol. Sci. 13 (8) (2012) 10257–10267.

[12] C. Li, Y. Meng, Z. Ying, N. Xu, D. Hao, M. Gao, W. Zhang, L. Xu, Y. Gao, X. Ying, Three novel alkaloids from *Portulaca oleracea* L. and their anti-inflammatory effects, J. Agric. Food Chem. 64 (29) (2016) 5837–5844.

[13] E.S. Al-Sheddi, N.N. Farshori, M.M. Al-Oqail, J. Musarrat, A.A. Al-Khedhairy, M.A. Siddiqui, *Portulaca oleracea* seed oil exerts cytotoxic effects on human liver cancer (HepG2) and human lung cancer (A-549) cell lines, Asian Pac. J. Cancer Prev. APJCP 16 (8) (2015) 3383–3387.

[14] Y. Bai, X. Zhang, J. Ma, G. Xu, Anti-diabetic effect of *Portulaca oleracea* L. Polysaccharide and its mechanism in diabetic rats, Int. J. Mol. Sci. 17 (8) (2016) 1201.

[15] A. Eidi, P. Mortazavi, J.Z. Moghadam, P.M. Mardani, Hepatoprotective effects of *Portulaca oleracea* extract against CCl4-induced damage in rats, Pharm. Biol. 53 (7) (2015) 1042–1051.

[16] K. Chan, M.W. Islam, R. Radhakrishnan, M.N. Zakaria, M. Habibullah, A. Attas, The analgesic and anti-inflammatory effects of *Portulaca oleracea* L. subsp. sativa (Haw.) Celak, J. Ethnopharmacol. 73 (3) (2000) 445–451.

[17] M. Rafieian-Kopaei, S. Alesaeidi, *Portulaca oleracea*: a review study with anti-inflammatory and muscle relaxant perspective, Indian J Med Res Pharm Sci 3 (11) (2016) 50–56.

[18] M.S.Z. Jan, W. AhmadAbdullah, A. Kamil, M.A. Khan, M.U. Rehman, I. Ullah, M.S. Jan, Protective effect of the solvent extracts of *Portulacca oleracea* against acidified ethanol induced gastric ulcer in rabbits.Drug, Chem. Toxicol 45 (1) (2022) 301–310.

[19] A.E.A. Moneim, M.A. Dkhil, S. Al-Quraishy, The potential role of *Portulaca oleracea* as a neuroprotective agent in rotenone-induced neurotoxicity and apoptosis in the brain of rats, Pestic Biochem Phys 105 (3) (2013) 203–212.

[20] J. Guo, J. Peng, J. Han, K. Wang, R. Si, H. Shan, X. Wang, J. Zhang, Extracts of *Portulaca oleracea* promote wound healing by enhancing angiology regeneration and inhibiting iron accumulation in mice, Chin Herb Med 26 (2) (2022) 263–272.

[21] X. Lei, J. Li, B. Liu, N. Zhang, H. Liu, Separation and identification of Four New compounds with antibacterial activity from *Portulaca oleracea* L, Molecules 20 (9) (2015) 16375–16387.

[22] C. Di Lorenzo, F. Colombo, S. Biella, C. Stockley, P. Restani, Polyphenols and human health: the role of bioavailability, Nutrients 13 (1) (2021) 273.

[23] A.Z. Barakat, R.I. Bassuiny, A.M. Abdel-Aty, S.A. Mohamed, Diabetic complications and oxidative stress: the role of phenolic-rich extracts of saw palmetto and date palm seeds, J. Food Biochem. 44 (11) (2020) e13416.

[24] M. Messaoudi, A. Rebiai, B. Sawicka, M. Atanassova, H. Ouakouak, I. Larkem, C. Egbuna, C.G. Awuchi, S. Boubekeur, M.A. Ferhat, S. Begaa, N. Benchikha, Effect of extraction methods on polyphenols, flavonoids, mineral elements, and biological activities of essential oil and extracts of *Mentha pulegium* L, Molecules 27 (1) (2021) 11.

[25] M.F. Lubis, P.A.Z. Hasibuan, H. Syahputra, R. Astyka, I. Baruna, Phytochemical profile and pharmacological activity of *Vernonia amygdalina* delile stem bark extracts using different solvent extraction, OAMJMS 10 (A) (2022) 860–866.

[26] A.M. Abdel-Aty, A.M. Elsayed, H.A. Salah, R.I. Bassuiny, S.A. Mohamed, Egyptian chia seeds (*Salvia hispanica* L.) during germination: upgrading of phenolic profile, antioxidant, antibacterial properties and relevant enzymes activities, Food Sci. Biotechnol. 30 (2021) 723–734.

[27] M.F. Lubis, P.A.Z. Hasibuan, H. Syahputra, J.M. Kelait, V.E. Kaban, R. Astyka, Duku (*Lansium domesticum*) leaves extract induces cell cycle arrest and apoptosis of HepG2 cells via PI3K/Akt Pathways, Trends Sci 20 (2) (2023) 6437, 6437.

[28] T. Lefebvre, E. Destandau, E. Lesellier, Selective extraction of bioactive compounds from plants using recent extraction techniques: a review, J. Chromatogr. A 1635 (2021) 461770.

[29] A. Oreopoulou, D. Tsimogiannis, V. Oreopoulou, Extraction of polyphenols from aromatic and medicinal plants: an overview of the methods and the effect of extraction parameters, Polyphenols in plants (2019) 243–259.

[30] N. Alonso-Carrillo, M.D. Aguila-Santamaria, E.J. Vernon-Carter, R. Jimenez-Alvarado, F. Cruz-Sosa, A. Roman-Guerrero, Extraction of phenolic compounds from *Satureja macrostema* using microwave-ultrasound assisted and reflux methods and evaluation of their antioxidant activity and cytotoxicity, Ind. Crops Prod. 103 (2017) 213–221.

[31] Y. Ma, A. Meng, P. Liu, Y. Chen, A. Yuan, Y. Dai, K. Ye, Y. Yang, Y. Wang, Z. Li, Reflux extraction optimization and antioxidant activity of phenolic compounds from *Pleioblastus amarus* (Keng) shell, Molecules 27 (2) (2022) 362.

[32] M.L. Moldovan, S. Iurian, C. Puscas, R. Silaghi-Dumitrescu, D. Hanganu, C. Bogdan, L. Vlase, I. Oniga, D. Benedec, A design of experiments Strategy to enhance the recovery of polyphenolic compounds from *Vitis vinifera* by-products through heat reflux extraction, Biomolecules 9 (10) (2019) 529.

[33] M.A. Bezerra, R.E. Santelli, E.P. Oliveira, L.S. Villar, L.A. Escaleira, Response surface methodology (RSM) as a tool for optimization in analytical chemistry, Talanta 76 (5) (2008) 965–977.

[34] M. Yolmeh, S.M. Jafari, Applications of response surface methodology in the food industry processes, Food Bioprocess Technol. 10 (2017) 413–433.

[35] C. Liyana-Pathirana, F. Shahidi, Optimization of extraction of phenolic compounds from wheat using response surface methodology, Food Chem. 93 (1) (2005) 47–56.

[36] G. Difonzo, G. Squeo, A. Pasqualone, C. Summo, V.M. Paradiso, F. Caponio, The challenge of exploiting polyphenols from olive leaves: addition to foods to improve their shelf-life and nutritional value, J. Sci. Food Agric. 101 (8) (2021) 3099–3116.

[37] M.I. Dias, I.C. Ferreira, M.F. Barreiro, Microencapsulation of bioactives for food applications, Food Funct. 6 (4) (2015) 1035–1052.

[38] A.F.M. Bora, S. Ma, X. Li, L. Liu, Application of microencapsulation for the safe delivery of green tea polyphenols in food systems: review and recent advances, Food Res. Int. 105 (2018) 241–249.

[39] M. Banožić, J. Vladić, I. Banjari, D. Velić, K. Aladić, S. Jokić, Spray drying as a method of choice for obtaining high quality products from food wastes– A review, Food Rev. Int. 39 (4) (2023) 1953–1985.

[40] C.G. Drosou, M.K. Krokida, C.G. Biliaderis, Encapsulation of bioactive compounds through electrospinning/electrospraying and spray drying: a comparative assessment of food-related applications, Dry. Technol. 35 (2) (2017) 139–162.

[41] V.R. de Sousa, A. Marcelo da Cunha Santos, B. Viana de Sousa, G. de Araújo Neves, L. Navarro de Lima Santana, R.R. Menezes, A review on chitosan's uses as biomaterial: tissue engineering, drug delivery systems and cancer treatment, Materials 13 (21) (2020) 4995.

[42] M.A.S. Abourehab, S. Pramanik, M.A. Abdelgawad, B.M. Abualsoud, A. Kadi, M.J. Ansari, A. Deepak, Recent advances of chitosan formulations in biomedical applications, Int. J. Mol. Sci. 23 (18) (2022) 10975.

[43] A.A. Alzandi, D.M. Naguib, A.M. Abas, Onion extract encapsulated on nano chitosan: a promising anticancer agent, J. Gastrointest. Cancer 53 (1) (2021) 211–216.

[44] A.J. Jorge, D.L.G.T. Heliodoro, Z.C. Alejandro, B.C. Ruth, A.C. Noé, The optimization of phenolic compounds extraction from cactus pear (*Opuntia ficus-indica*) skin in a reflux system using response surface methodology, Asian Pac. J. Trop. Biomed. 3 (6) (2013) 436–442.

[45] M.F. Lubis, H. Syahputra, D.N. Illian, V.E. Kaban, Antioxidant activity and nephroprotective effect of *Lansium parasiticum* leaves in doxorubicin-induced rats, J Res Pharm 26 (3) (2022) 565–573.

[46] N. Siddiqui, V. Aeri, Optimization of Betulinic acid extraction from *Tecomella undulata* bark using a Box-Behnken design and its Densitometric validation, Molecules 21 (4) (2016) 393.

[47] A. Trifan, G. Zengin, K.I. Sinan, E. Wolfram, K. Skalicka-Woźniak, S.V. Luca, LC-HRMS/MS phytochemical profiling of *Symphytum officinale* L. and *Anchusa ochroleuca* M. Bieb. (Boraginaceae): unveiling their multi-biological potential via an integrated approach, J. Pharm. Biomed. Anal. 10 (204) (2021) 114283.

[48] P. Vonghirundecha, S. Chusri, P. Meunprasertdee, T. Kaewmanee, Microencapsulated functional ingredients from a *Moringa oleifera* leaf polyphenol-rich extract: characterization, antioxidant properties, in vitro simulated digestion, and storage stability, LWT 154 (2022) 112820.

[49] M. Ghobadi, A. Koocheki, M.J. Varidi, M. Varidi, Encapsulation of curcumin using Grass pea (*Lathyrus sativus*) protein isolate/*Alyssum homolocarpum* seed gum complex nanoparticles, Innovat. Food Sci. Emerg. Technol. 72 (2021) 102728.

[50] B. da Silva Soares, R.P. Siqueira, M.G. de Carvalho, J. Vicente, E.E. Garcia-Rojas, Microencapsulation of sacha inchi oil (*Plukenetia volubilis* L.) using complex coacervation: formation and structural characterization, Food Chem. 15 (298) (2019) 125045.

[51] W. Cichocki, A. Czerniak, K. Smarzynski, O. Jezowski, D. Kmiecik, H.M. Baranowska, K. Walkowiak, E. Ostrowska-Ligeza, M.B. Rozanska, M. Lesiecki, P. L. Kowalczewski, Physicochemical and morphological study of the *Saccharomyces cerevisiae* cell-based microcapsules with novel cold-pressed oil blends, Appl. Sci. 12 (13) (2022) 6577.

[52] H. Widodo, S. Sismindari, W. Asmara, A. Rohman, Antioxidant activity, total phenolic and flavonoid contents of selected medicinal plants used for liver diseases and its classification with chemometrics, J. Appl. Pharmaceut. Sci. 9 (6) (2019) 99–105.

[53] M. Soltanzadeh, S.H. Peighambardoust, B. Ghanbarzadeh, M. Mohammadi, J.M. Lorenzo, Chitosan nanoparticles as a promising nanomaterial for encapsulation of pomegranate (*Punica granatum* L.) peel extract as a natural source of antioxidants, Nanomaterials 11 (6) (2021) 1439.

[54] U. Harahap, A. Dalimunthe, T. Hertiani, M. MuhammadNasri, D. Satria, Antioxidant and antibacterial activities of ethanol extract of *Vernonia amygdalina* Delile. Leaves, AIP Conf. Proc. 2342 (1) (2021) 080011.

[55] H.J. Choi, M. Naznin, M.B. Alam, A. Javed, F.H. Alshammari, S. Kim, S.H. Lee, Optimization of the extraction conditions of *Nypa fruticans* Wurmb. using response surface methodology and artificial neural network, Food Chem. 381 (2022) 132086.

[56] S. Sedraoui, A. Badr, M.G.M. Barba, A. Doyen, Z. Tabka, Y. Desjardins, Optimization of the ultrahigh-pressure–assisted extraction of phenolic compounds and antioxidant activity from palm dates (*Phoenix dactylifera L.*), Food Anal. Methods 13 (10) (2020) 1556–1569.

[57] A. Oreopoulou, D. Tsimogiannis, V. Oreopoulou, Extraction of polyphenols from aromatic and medicinal plants: an overview of the methods and the effect of extraction parameters, Polyphenols in plants (2019) 243–259.

[58] J. Xi, L. He, L. Yan, Kinetic modeling of pressure-assisted solvent extraction of polyphenols from green tea in comparison with the conventional extraction, Food Chem. 166 (2014) 287–291.

[59] G.J. Swamy, A. Sangamithra, V. Chandrasekar, Response surface modeling and process optimization of aqueous extraction of natural pigments from Beta vulgaris using Box–Behnken design of experiments, Dyes Pigments 111 (2014) 64–74.

[60] L.M.B. Ferreira, A.M. Dos Santos, F.I. Boni, K.C. Dos Santos, L.M.G. Robusti, M.P.C. de Souza, N.N. Ferreira, S.G. Carvalho, V.M.O. Cardoso, M. Chorilli, B.S. F. Cury, D.R.M. de Godoi, M.P.D. Gremião, Design of chitosan-based particle systems: a review of the physicochemical foundations for tailored properties, Carbohydr. Polym. 250 (2020) 116968.

[61] M. Fan, Q. Hu, K. Shen, Preparation and structure of chitosan soluble in wide pH range, Carbohydr. Polym. 78 (1) (2009) 66–71.

[62] T.A. Ahmed, B.M. Aljaeid, Preparation, characterization, and potential application of chitosan, chitosan derivatives, and chitosan metal nanoparticles in pharmaceutical drug delivery, Drug Des. Dev. Ther. 10 (2016) 483–507.

[63] M. Yousefi, N. Khorshidian, A.M. Mortazavian, K. Khosravi-Darani, Preparation optimization and characterization of chitosan-tripolyphosphate microcapsules for the encapsulation of herbal galactagogue extract, Int. J. Biol. Macromol. 140 (2019) 920–928.

[64] M. Yousefi, V.G. Mohammadi, M. Shadnoush, N. Khorshidian, A.M. Mortazavian, *Zingiber officinale* essential oil-loaded chitosan-tripolyphosphate nanoparticles: fabrication, characterization and in-vitro antioxidant and antibacterial activities, Food Sci. Technol. 28 (7) (2022) 592–602.

[65] N. Khorshidian, A. Mahboubi, N. Kalantari, H. Hosseini, M. Yousefi, M. Arab, A.G. da Cruz, A.M. Mortazavian, F.S. Mahdavi, Chitosan-coated alginate microcapsules loaded with herbal galactagogue extract: formulation optimization and characterization, Iran. J. Pharm. Res. (IJPR) 18 (3) (2019) 1180–1195.

[66] R.A. Hashad, R.A. Ishak, S. Fahmy, S. Mansour, A.S. Geneidi, Chitosan-tripolyphosphate nanoparticles: optimization of formulation parameters for improving process yield at a novel pH using artificial neural networks, Int. J. Biol. Macromol. 86 (2016) 50–58.

[67] J. Antoniou, F. Liu, H. Majeed, J. Qi, W. Yokoyama, F. Zhong, Physicochemical and morphological properties of size-controlled chitosan–tripolyphosphate nanoparticles, Colloids Surf., A: Physicochem Eng 465 (2015) 137–146.

[68] T.G. do Nascimento, N.M. do Nascimento, A.S. Ribeiro, C.P. de Almeida, J.I.Z. dos Santos, I.D. Basilio-Junior, F.G. Calheiros-Silva, G.M. Lira, P.B. Escodro, I.C. C. de Mores Porto, V.A. da Silva, C.B. Dornelas, J. dos Santos Sousa, J.D. de Freitas, Preparation and characterization of chitosanates loaded with Brazilian red propolis extract, J. Therm. Anal. Calorim. 147 (2021) 7837–7848.

[69] M. Iannone, R. Mare, D. Paolino, A. Gagliardi, F. Froiio, D. Cosco, M. Fresta, Characterization and in vitro anticancer properties of chitosan-microencapsulated flavan-3-ols-rich grape seed extracts, Int. J. Biol. Macromol. 104 (Pt A) (2017) 1039–1045.

[70] S.C.S.R. de Moura, C.L. Berling, S.P.M. Germer, I.D. Alvim, M.D. Hubinger, Encapsulating anthocyanins from *Hibiscus sabdariffa* L. calyces by ionic gelation: pigment stability during storage of microparticles, Food Chem. 241 (241) (2017) 317–327.

[71] S. Thuekeaw, T. Buwjoom, B. Maneewan, C. Nuengjamnong, Porous alginate microcapsule-containing sweet basil oil (*Ocimum basilicum*) generated by gas foaming with ionic gelation as an efficient antioxidant delivery in stimulated poultry gastrointestinal tract, ACS Food Sci Technol 3 (12) (2023) 2078–2084.

[72] T.K. Shah, A. Kumar, R. Tandel, R.A.H. Bhat, D. Sarma, Identification of functional groups in *Thymus linearis* ethanol leaf extract through fourier transform infrared spectroscopy (FTIR), J. Pharmacogn. Phytochem. 8 (4) (2019) 3013–3015.

[73] A.L. Parizel, H.K. Stulzer, M.C.M. Laranjeira, I.M.d. Brighente, T.C.R. de Souza, Evaluation of chitosan microparticles containing curcumin and crosslinked with sodium tripolyphosphate produced by spray drying, Quím. Nova 35 (2012) 1127–1132.

[74] K. Chen, M. Zhang, A.S. Mujumdar, M. Wang, Quinoa protein isolate-gum Arabic coacervates cross-linked with sodium tripolyphosphate: characterization, environmental stability, and Sichuan pepper essential oil microencapsulation, Food Chem. 404 (Pt A) (2023) 134536.

[75] J.S. Boeing, E.O. Barizão, B.C. E Silva, P.F. Montanher, V. de Cinque Almeida, J.V. Visentainer, Evaluation of solvent effect on the extraction of phenolic compounds and antioxidant capacities from the berries: application of principal component analysis, Chem. Cent. J. 8 (1) (2014) 48.

[76] S. Phupaboon, M. Matra, R. Prommachart, P. Totakul, C. Supapong, M. Wanapat, Extraction, characterization, and chitosan microencapsulation of bioactive compounds from *Cannabis sativa* L., *Cannabis indica* L., and *Mitragyna speiosa* K, Antioxidants 11 (11) (2022) 2103.

[77] F.R. Abrahao, L.C.R. Rocha, T.A. Santos, E.L. do Carmo, L.A.S. Pereira, S.V. Borges, R.G.F.A. Pereira, D.A. Botrel, Microencapsulation of bioactive compounds from espresso spent coffee by spray drying, LWT 103 (23) (2018) 116–124.